Measuring the Electron Mass through Compton Scattering

Gopal K. Goel*
MIT Department of Physics
(Dated: May 10, 2023)

We measure the Compton scattering of 661.6 keV gamma rays and measure the energies of the scattered gamma ray and the recoiled electron. We fit our results to Compton's theory of light-electron scattering, and in the process measure the mass of the electron to be 537 ± 25 keV, which matches the accepted value of 511 keV.

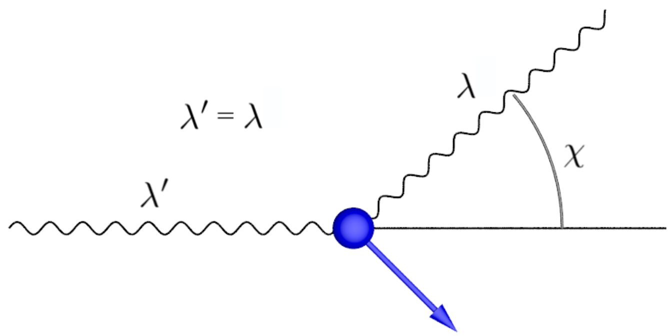

FIG. 1. Schematic depiction of Thomson Scattering. Taken from https://commons.wikimedia.org/wiki/File:Thomson-scattering.png

I. MOTIVATION AND THEORETICAL DESCRIPTION

I.1. Historical Background

The main physical process of interest in this paper is the elastic scattering of light off an electron. The celebrated physicist J.J. Thomson analyzed this process in the early twentieth century using classical electromagnetic theory and proved that the wavelength of the emitted radiation must be equal to the wavelength of the incident radiation [1]. The basic idea is that the oscillating electromagnetic fields of the incident radiation cause the electron to oscillate, and since accelerating charged particles emit radiation, the electron emits radiation in all directions, with a certain differential cross section. As previously mentioned, Thomson utilized Maxwell's equations to demonstrate that the wavelength of the emitted radiation in this process matches that of the incident radiation. See Figure 1 for a schematic depiction of this process.

In 1923, A.H. Compton showed that for high energy incident radiation, the wavelength of the emitted light was actually longer than the wavelength of the incident light. As was the case for many early twentieth century discoveries, the solution was based on the quantum nature of light. By treating the incident radiation as a particle-like photon and using Einstein's special relativity, Compton was able to derive a theoretical prediction for the wavelength shift.

Our goal in this paper is to provide evidence for Compton's theory of light-electron scattering, and in the process extract a value for the mass of the electron.

I.2. Derivation of wavelength shift in Compton Scattering

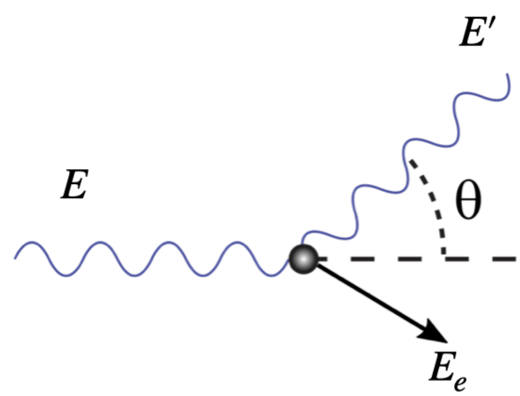

FIG. 2. Schematic depiction of Compton Scattering. Modified from https://upload.wikimedia.org/wikipedia/commons/e/e3/Compton-scattering.svg

Restrict attention to light scattered at an angle θ, as shown in Figure 2. Let E be the energy of the incoming photon, E' be the energy of the scattered photon, and let E_e be the energy of the post-scattering electron. Let m_e be the mass of the electron, and temporarily set $c = 1$. The energy-momentum four-vector of the incident photon is $(E, E, 0)$, and the energy-momentum four-vector of the scattered photon is $(E', E' \cos\theta, E' \sin\theta)$. Therefore, the energy-momentum four-vector of the scattered electron is $(E - E' + m_e, E - E' \cos\theta, -E' \sin\theta)$, so

$$(E - E' + m_e)^2 - (E - E' \cos\theta)^2 - (-E' \sin\theta)^2 = m_e^2.$$

* gopalkg@mit.edu

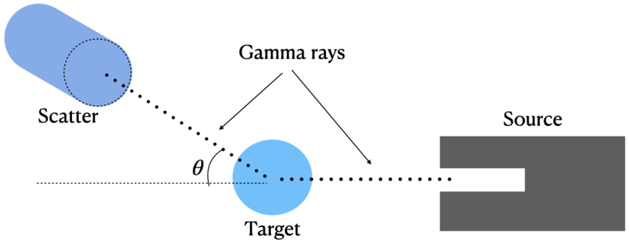

FIG. 3. Schematic depiction of our setup

Simplifying this equation and reintroducing c, we find that

$$\frac{1}{E'} - \frac{1}{E} = \frac{1}{m_e c^2}(1 - \cos\theta). \tag{1}$$

We set E to be some fixed value, and measure E' at various angles θ. By fitting the data to (1), we will be able to extract a value for m_e, the mass of the electron.

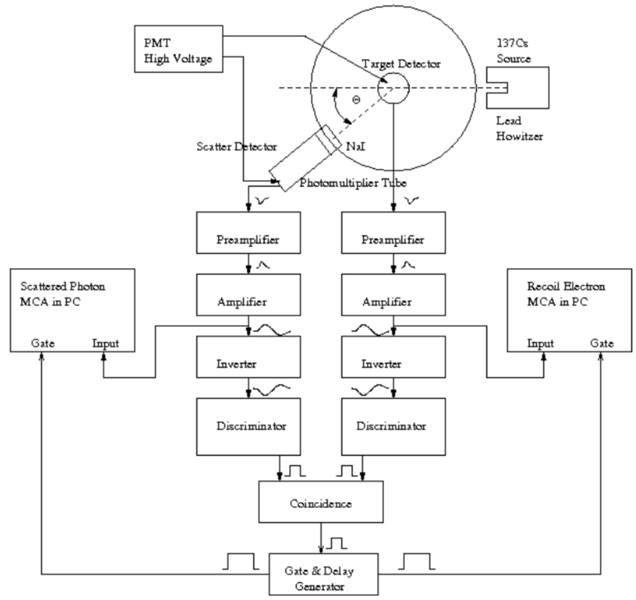

FIG. 4. Electronic setup schematic. Taken from [2]

II. EXPERIMENTAL SETUP

We use gamma rays generated from the radioactive source ^{137}Cs, which has a strong photopeak at 661.6 keV, and we use two detectors, which are NaI scintillation counters. The energy of the incident gamma rays are high enough such that the primary interaction between the gamma rays and the scintillator is Compton scattering.

The ^{137}Cs is placed in a lead howitzer such that we get a collimated beam of gamma rays. The first detector, the *target detector*, is placed vertically directly in the line of sight of the gamma rays. The second detector, the *scatter detector*, is placed horizontally at a variable angle. The setup is shown in Figure 3.

Given a Compton scattering event in the target detector, the target detector registers a count with energy E_e of the scattered electron, and the scatter detector registers a count with energy E', the energy of the scattered photon. In order to only pick up events that correspond to scattering at the specific angle θ, we set up coincidence counting between the detectors, so counts are registered only when both detectors measure an event at essentially the exact same time. Since the scattered photon travels at the speed of light, the time between the two events is effectively instantaneous, which is why coincidence counting restricts to Compton scattering events at angle θ.

In order to restrict to coincidences, we send the detector outputs through a series of electronic transformations. The basic idea is to convert the analog signal of a detection (which looks like some smooth bump) into a sharp square wave (through an amplifier, inverter, and discriminator), and use a coincidence detector to measure when these two sharp square wave signals overlap, corresponding to a coincidence. We analyze the outputs of the detectors in a multichannel analyzer (MCA), which presents the counts in a histogram format, binned based on the energy registered by the detector. The full electronic setup is depicted in Figure 4.

Given a working coincidence setup, the functionality of the software is as follows. We can turn coincidence restriction on or off through the software, and for each detector, the software outputs a histogram of counts at each channel number. The channel number roughly corresponds to energy, but the correspondence needs to be established, so we have to use known values to construct a calibration fit to turn channel number into energy values.

III. MCA CALIBRATION

In order to calibrate the MCA software, we use radioactive sources that produce photopeaks at known energies, and use a linear fit between energy and channel number. Note that the calibration for the target detector and the scatter detector will be different.

We use a combination of the 661.6 keV peak of ^{137}Cs, the 511 keV peak of ^{22}Na, and the $81, 302, 356$ keV peaks of ^{133}Ba. We place the radioactive source between the target and scatter detector, and turn off coincidence, so that we get strong peaks in both detectors. The measured spectra of the various radioactive sources in the two detectors is shown in Figure 5.

We use a linear fit

$$N = \alpha E + \beta$$

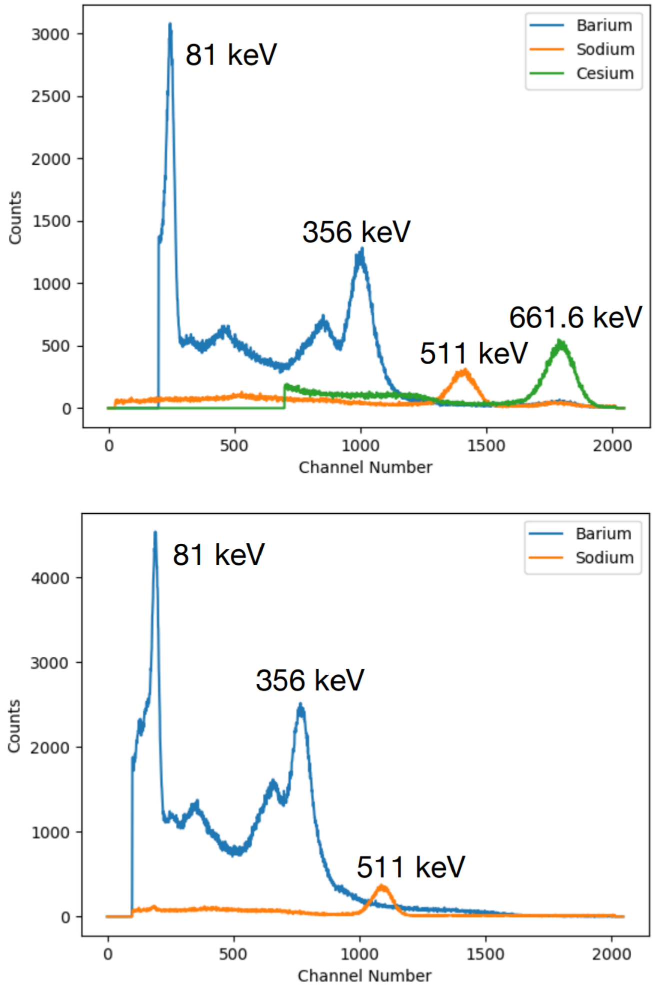

FIG. 5. Spectra of calibration sources with labeled true peaks. Target detector is shown on top, and scatter detector is shown on bottom.

between channel number and energy. Using χ^2 fitting, we obtain fit parameters

$$\alpha = [2.68 \pm 0.03]\frac{\text{channels}}{\text{keV}}, \quad \beta = 24 \pm 6 \text{ channels}$$

for the target detector, and

$$\alpha = [2.11 \pm 0.03]\frac{\text{channels}}{\text{keV}}, \quad \beta = 16 \pm 10 \text{ channels}$$

for the scatter detector. The linear fits along with the χ^2 and p-values are shown in Figure 6.

IV. DATA AND ANALYSIS

We let the setup run at angles

$$\theta = 30^\circ, 60^\circ, 90^\circ, 135^\circ, 150^\circ$$

for multi-day exposures. The goal is to extract values for E' at each of these angles, in order to compare to (1). To do this, we need a heuristic for what the spectra of the two detectors should look like.

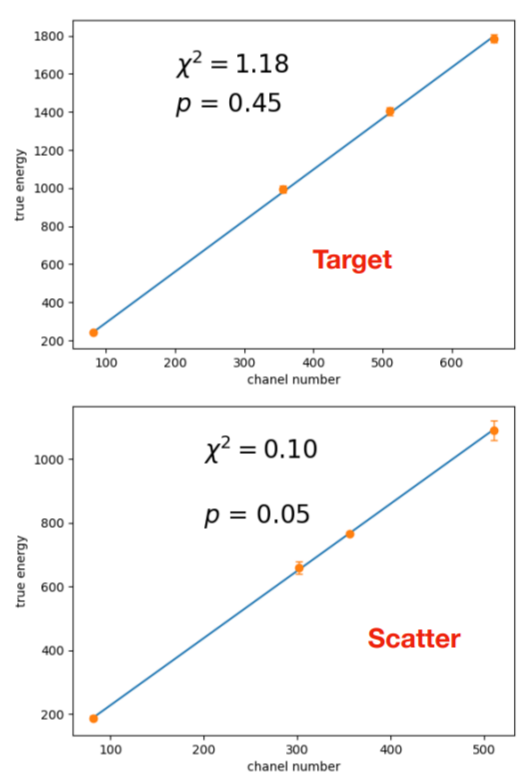

FIG. 6. Calibration fit of the target and scatter detectors along with χ^2 and p values for the fit.

In order to construct a useful model for what the spectra should look like, we need to take into account the fact that restricting to coincidences will not fully restrict to Compton events with scattering angle θ.

In the scatter spectrum, we expect to see a strong peak at energy E', since most of the gamma rays entering the scatter detector are coming from Compton scattering at angle θ. Temporarily ignoring coincidence, we expect to see a strong peak at energy E in the target spectrum, which corresponds to incident gamma rays directly registering in the detector, and we expect to see a relatively flat *Compton spectrum*, which corresponds to all possible energies E_e allowed by Compton scattering. The maximum E_e allowed can be calculated from (1) and the relation $E_e = E - E'$, and we expect to see a fall off in the spectrum at this maximum value. This is known as the *Compton edge*. Accounting now for the fact that a large fraction of coincidence events correspond to Compton scattering at the specific angle θ, we expect to see a peak at E_e on top of the previously described target detector spectrum, as a disproportionally large fraction of our events are now Compton scattering at the specific angle θ. These heuristics are depicted in Figure 7.

The measured spectrum for $\theta = 60^\circ$ is shown in Figure 8. The peak channel number value is measured by computing the median channel for the peak, and the sta-

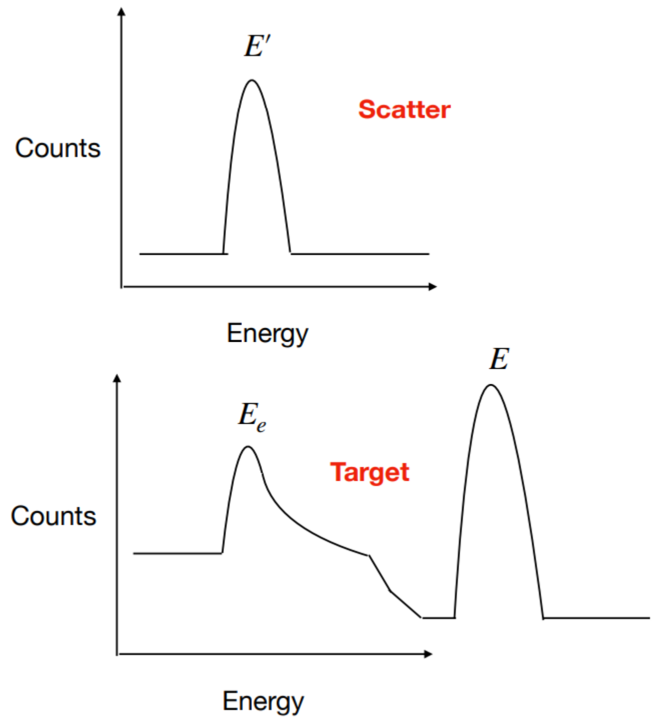

FIG. 7. General expected structure of detector spectra.

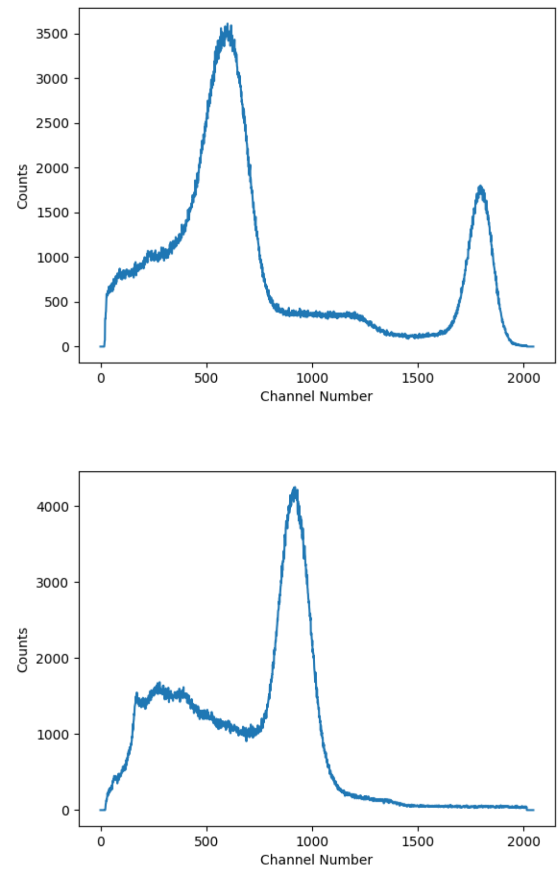

FIG. 8. Measured spectra for $\theta = 60°$, with target on top and scatter on bottom.

tistical uncertainty is calculated by estimating the range where the peak is relatively flat within Poisson fluctuation. We then use the calibration fit to estimate the peak energy value. The systematic uncertainty in E' arises from the uncertainty in the calibration, which is a fixed systematic potential error. Not all measurements were as clean as the $\theta = 60°$ run, so some of the relevant peaks were not extractable. The measured values are shown in the following table. The statistical uncertainty is shown followed by the systematic uncertainty arising from calibration.

θ	E_e (keV)	E' (keV)
30°	$61 \pm 9 \pm 5$	$561 \pm 9 \pm 8$
60°	$214 \pm 9 \pm 5$	$425 \pm 5 \pm 6$
90°	N/A	$294 \pm 19 \pm 4$
135°	$412 \pm 15 \pm 5$	$191 \pm 9 \pm 3$
150°	$421 \pm 15 \pm 5$	N/A

As a cross-check, we find that $E_e + E'$ is between $0.9E$ and $0.95E$ for the three angles where we have both values. We expect to find $E_e + E' = E$, so there is some systematic downward shift in E_e which we don't have a good explanation of, but regardless this more or less confirms our identifications of the peaks.

We perform a χ^2 linear fit of $1/E'$ against $1 - \cos\theta$ as per (1). The linear fit along with χ^2 and p-values is shown in Figure 9. The curve fit gives us values for $\frac{1}{m_e c^2}$ and $\frac{1}{E}$, so taking the reciprocal, we find results of

$$E = 675 \pm 25 \text{ keV}$$
$$m_e c^2 = 537 \pm 25 \text{ keV}.$$

V. DISCUSSION

The measured values shown above match the known values within error, which are $E = 661.6$ keV and $m_e c^2 = 511$ keV. This provides strong evidence for Compton's quantum theory of light-electron scattering over Thomson's classical theory, which gives further evidence for the quantum nature of light.

In order to capture systematic uncertainty, we need to properly understand why $E' + E_e$ is consistently lower than E by about 5–10%. We suspect that this systematic error is mostly in the E_e peak, which means it wouldn't affect our analysis, but we don't have concrete evidence for this claim. Furthermore, our electrical setup broke several times due to a faulty discriminator, so our calibration has potential to be off from run to run. We benchmarked the calibration between runs, so this is likely not

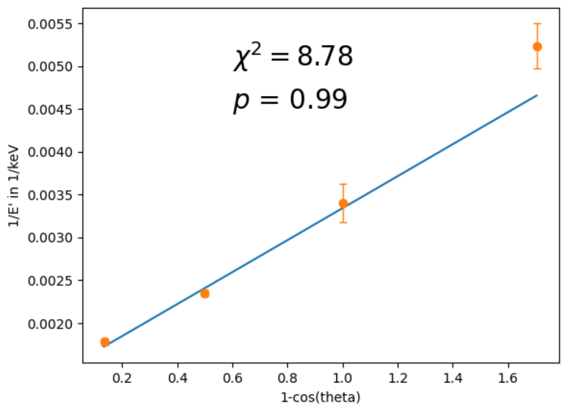

FIG. 9. Linear fit of $1/E'$ against $1 - \cos\theta$

an issue, but a more careful analysis would require a more consistent electrical setup.

ACKNOWLEDGEMENTS

Thanks to my partner O.C. Dugan, and all the JLab staff, particularly Dr. Levine and Dr. Robinson.

[1] *Conduction of electricity through gases.* Thomson, J.J. Cambridge University Press (1906).

[2] *Compton Scattering.* MIT Department of Physics (2013).